2800 Days of Monitoring the Timing of PSR B1509-58 with RXTE

Arnold H. Rots

Harvard-Smithsonian Center for Astrophysics, 60 Garden Street MS 67, Cambridge, MA 01238, USA

Abstract. We have analyzed 90 observations of the young pulsar B1509-58 made by RXTE over 7.6 years.

The pulse profile can be described as a combination of two systems. The first consists of two narrow components separated by 0.14 period with an amplitude ratio of 10:3; the second consists of a single broader component. The two systems appear to be shifting with respect to each other as a function of energy.

We have derived a single timing ephemeris on the basis of the X-ray observations, using terms up to the third derivative. There is no indication that a fourth derivative is required. The resulting value of the first braking index is consistent with that derived from radio observations, but the second braking index is twice its expected value. This casts some doubt on the significance of the pulsar's characteristic age (1700 years).

The phase residuals have been fit with sine components, resulting in an estimate of the proper motion (45±25 mas/yr at a position angle of 45±45°) and of masses and orbital radii (ranging from 0.7 to 2 AU and 0.25 to 2.5 earth masses) of planetary material - if that is the cause of these phase excursions.

INTRODUCTION

The young energetic pulsar PSR B1509-58 was initially discovered in X-rays (Seward & Harnden 1982) and subsequently at radio frequencies. It has a period of 150 ms, is extremely stable (no glitches over 20 years), exhibits a fair amount of timing noise, and has a characteristic age of 1700 yr. However, there is a discrepancy between this age and the assumed age of the associated supernova remnant, G320.4-1.2, which is commonly estimated at 104 yr. For more specifics, see Kaspi et al. (1994) and Gaensler et al. (2002).

ANALYSIS

All data have been processed with the program *faseBin* (which forms the core of HEASARC's *Ftool fasebin*), using only the top layer events in the energy range 2-16 keV, and applying RXTE fine clock corrections resulting in an absolute time accuracy < 8 ms.

We started out with the radio timing ephemeris provided by ATNF, based on JPL solar system ephemeris DE200, but subsequently bootstrapped to a timing ephemeris based on the RXTE data themselves, using DE405.

The analysis produced three products: a pulse profile template, a single timing ephemeris covering the entire 7.6 year period, and the phase residuals as a function of time.

The pulse profile template was developed in three stages. The average profile of the first 10 observations was used to determine the phases of the first 60 observations through cross-correlation. The pulse profiles of those observations were then shifted to provide a provisional template which was used to determine the phases of the first 87 observations more accurately, leading to a definitive template consisting of three Gaussians. From there on, the phase has been defined as the phase of the main component.

The timing ephemeris is derived by successive improvement, fitting fourth order polynomials to the phase residuals.

PULSE PROFILE

The pulse profile and a fit consisting of three Gaussian functions is shown in Fig. 1. The fit parameters are given in Table 1. The resultant reduced χ^2 is 1.6.

A schematic interpretation of the pulse profile is that it consists of a pair of narrow components (1 and 3) and a wider component (2) that is responsible to the "hump" on the profile. The narrow components are very similar in width (FWHM 0.137), have a constant phase difference (0.140), and a constant amplitude ratio (10:3). The wide component has a FWHM of 0.334 and is roughly coincident with the second narrow component, but appears

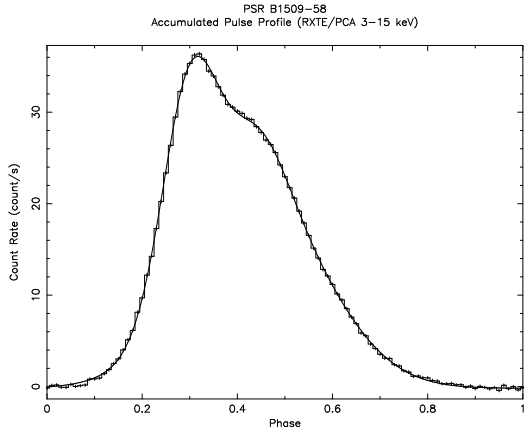

FIGURE 1. Average pulse profile with three-Gaussian fit (see Table 1)

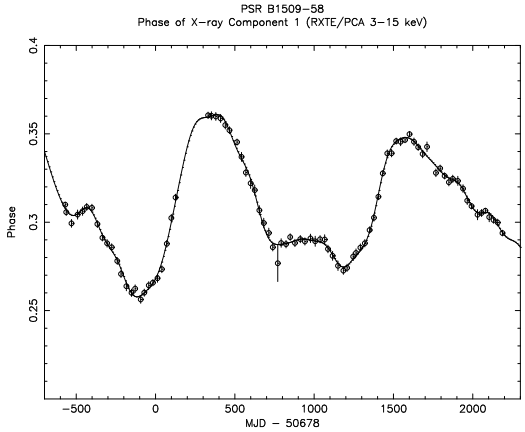

FIGURE 2. Phase residuals as a function of time; see text and Table 3 for fitted function

to be moving toward earlier phases with respect to the system of narrow components, as energy increases; that change in (relative) phase appears proportional to $E^{-0.08}$. The wide component contains 63% of the pulsed power.

The template used to fit individual observations has fixed dispersions of 0.0579 for components 1 and 3 and 0.141 for component 2; it forces components 2 and 3 to be coincident in phase; and it sets the amplitude of component 3 at 0.3 times the amplitude of component 1. The resulting reduction in the number of free parameters ensures greater stability in the phase residual determination.

In the following the phase of the pulse profile is defined as the phase of component 1.

TIMING EPHEMERIS

Starting from the radio timing ephemeris provided by ATNF, we have derived a timing ephemeris based on the X-ray data alone by bootstrapping: phase residuals were fit with a fourth order polynomial which incremented the timing ephemeris which, in turn provided new phase residuals. A quartic polynomial was sufficient to fit the residuals; no fourth derivative was needed. The resulting timing ephemeris is given in Table 2.

It should be noted that the position is different from the best available radio position (Gaensler et al. 1999) by more than 3σ.

The first deceleration parameter (braking index) n is in good agreement with theoretical expectation ($n = 3$) and with earlier determinations (2.837). The second braking index m is about twice what one would expect ($m = n(2n-1)$). Livingstone et al. (2003) analyzed 20 years of radio timing data and derived $m = 12.7$, consistent with n. It will require a careful analysis to reconcile the two values since our data appear inconsistent with the low third derivative presented by Livingstone et al. There is the possibility that their result is distorted by changes in the Dispersion Measure. Although there is clear evidence for such changes occurring, it seems unlikely that it could lead to discrepancies of this magnitude.

Be that as it may, our result indicates a decreasing magnetic field and casts some doubt on the validity of interpreting the characteristic age of the pulsar: it may well be significantly older than 1700 yr. It should be noted that Gaensler et al. (1999) have questioned, on good grounds, the 10,000 yr age estimate for SNR G320.4-01.2.

The book is not closed on this issue.

PHASE RESIDUALS

The final phase residuals have an amplitude of 0.05 period, or 8 ms, and are presented in Fig. 2. We have fit these data with a constant offset term, a proper motion function, and a collection of sinusoids. The fit is also presented in Fig. 2 and has a reduced χ^2 value of 1.07. The constant offset is 0.30925 ± 0.00024, the proper motion fit 45 ± 25 mas/yr at a position angle of $45 \pm 45^\circ$. The sine component parameters are given in Table 3. Components 2 and 4 are the first harmonics of components 1 and 3, respectively.

We are well aware that such fits are a risky business. Not only can in principle any function be fitted with a collection of sine components, but there is dangerous interplay between long period sinusoids and the higher order terms of the polynomial fit of the timing ephemeris. Nevertheless, there is clear periodic behavior in the phase residuals and we feel comfortable that we have identified the global minimum in parameter space.

The sinusoidal components could be interpreted as

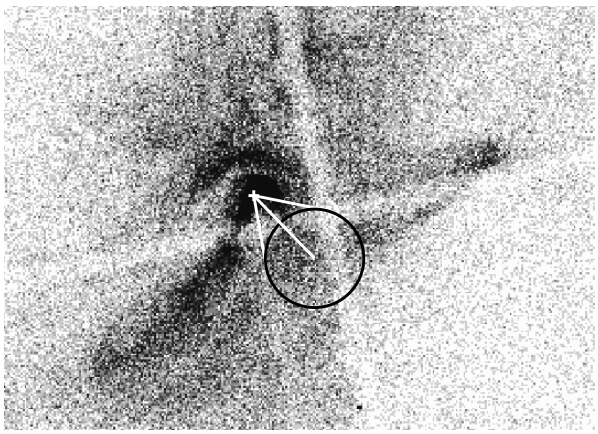

FIGURE 3. Chandra image (uncorrected for exposure) of PSR B1509-58. + marks the current position of the pulsar. The black circle shows the position 2000 yr ago, indicating the uncertainties of the fitted function. The white lines outline the bounds of the proper motion path over the past 2000 yr

gravitational in origin - either planets or clumps of ejecta. Table 4 provides the orbital elements and masses derived under that assumption. We would clearly be dealing with earth-like masses in earth-like orbits - except that they are highly eccentric. It is also plausible that the motions are caused by clumps of ejecta moving in unstable orbits that are not closed - giving rise to quasi-periodic residuals. Component 6 in Table 3 could possibly be explained as arising from Tkachenko (1966) oscillations. The fi t to the proper motion translates into a transverse velocity of 1100 km/s in a plane normal to the spin. Though that is unusual, it would be consistent with the kick mechanism proposed by Colpi & Wasserman (2002). The proper motion geometry is laid out in Fig. 3.

ACKNOWLEDGMENTS

We gratefully acknowledge the various discussions with and help from M. Bailes, B. Gaensler, K. Jahoda, V. Kaspi, and R. Manchester. This research has been supported by NASA grant NAG5-7335 and contract NAS 8-39073 (CXC).

REFERENCES

1. Colpi & Wasserman 2002, ApJ 581, 1271
2. Gaensler et al. 1999, MNRAS 305, 724
3. Gaensler et al. 2002, ApJ 569, 878
4. Kaspi et al. 1994, ApJ 422, L83
5. Livingstone, Kaspi & Manchester 2003, in IAU Symp. 218
6. Seward & Harnden 1982, ApJ 256, L45
7. Tkachenko 1966, Soviet Phys. JETP 23, 1049

TABLE 1. Pulse profile fitting parameters

Component	Central Phase	Dispersion	Amplitude
1	0.2996±0.0008	0.0576±0.0007	22.73±0.29
2	0.4430±0.0014	0.1418±0.0013	20.39±0.45
3	0.4407±0.0026	0.0596±0.0029	7.15±0.47

TABLE 2. Timing parameters for PSR B1509-58 (DE405)

Right Ascension (ICRS)	$15^h13^m55.640^s$	± 0.010
Declination(ICRS)	$-59°08'09.40''$	± 0.08
Epoch (MJD)	50678.000001153	UTC, geocenter
Frequency	6.6240222193327108	$\pm 4.4 \times 10^{-11}\mathrm{s}^{-1}$
First derivative	$-6.7302935510473 \times 10^{-1}1$	$\pm 2.6 \times 10^{-18}\mathrm{s}^{-2}$
Second derivative	$1.943319533 \times 10^{-21}$	$\pm 6.3 \times 10^{-26}\mathrm{s}^{-3}$
Third derivative	$-1.946814 \times 10^{-31}$	$\pm 2.1 \times 10^{-33}\mathrm{s}^{-4}$
First braking index n	2.8418	± 0.0002
$n(2n-1)$	13.310	± 0.001
Second braking index m	28.02	± 0.3

TABLE 3. Fit to phase residuals: sine components

Component	Period (d)	Amplitude (per.)	Phase offset (d)
1	1258.6 ± 11.3	0.03808 ± 0.00054	112.7 ± 8.8
2	629.3	0.01444 ± 0.00054	164.5 ± 8.9
3	889.6 ± 6.4	0.00907 ± 0.00037	84.4 ± 19.1
4	444.8	0.00486 ± 0.00037	24.4 ± 10.1
5	319.4 ± 14.3	0.00183 ± 0.00073	136.2 ± 38.8
6	213.0 ± 2.0	0.00171 ± 0.00034	141.9 ± 11.1
7	167.7 ± 1.9	0.00102 ± 0.00033	51.0 ± 13.5

TABLE 4. Planetary orbital elements and masses

Period (d)	Radius (AU)	Eccentricity	Mass $(m_{earth} \cdot \sin i\ )$
1258.6	2.552	0.93	2.105
889.6	2.025	0.84	0.632
319.4	1.023	< 0.9	0.252
213.0	0.781	< 0.9	0.309
167.7	0.666		0.216